GDCh Research Article Angewandte International Edition Chemie www.angewandte.org

How to cite: *Angew. Chem. Int. Ed.* **2024**, *63*, e202409134
doi.org/10.1002/anie.202409134

Supramolecular Chemistry

Unsymmetric Chiral Ligands for Large Metallo-Macrocycles: Selectivity of Orientational Self-Sorting

Ondřej Jurček, Subhasis Chattopadhyay, Elina Kalenius, Juha M. Linnanto, Anniina Kiesilä, Pia Jurček, Petr Radiměřský, and Radek Marek*

In memory of professor Erkki Kolehmainen, a great person and one of the pioneers of supramolecular chemistry of bile acids.

Abstract: Nature uses various chiral and unsymmetric building blocks to form substantial and complex supramolecular assemblies. In contrast, the majority of organic ligands used in metallosupramolecular chemistry are symmetric and achiral. Here we extend the group of unsymmetric chiral bile acids used as a scaffold for organic bispyridyl ligands by employing chenodeoxycholic acid (CDCA), an epimer of the previously used ursodeoxycholic acid (UDCA). The epimerism, flexibility, and bulkiness of the ligands leads to large structural differences in coordination products upon reaction with $Pd(NO_3)_2$. The UDCA-bispyridyl ligand self-assembles quantitatively into a single crown-like Pd_3L_6 complex, whereas the CDCA ligand provides a mixture of coordination complexes of general formula Pd_nL_{2n}, i.e., Pd_2L_4, Pd_3L_6, Pd_4L_8, Pd_5L_{10}, and even Pd_6L_{12} containing an impressive 120 chiral centers. The coordination products were studied by a combination of analytical methods, with ion-mobility mass spectrometry (IM-MS) providing valuable details on their structure and allowed an effective separation of *m/z* 1461 to individual signals according to the arrival time distribution, thereby revealing four different ions of $[Pd_3L_6(NO_3)_3]^{3+}$, $[Pd_4L_8(NO_3)_4]^{4+}$, $[Pd_5L_{10}(NO_3)_5]^{5+}$, and $[Pd_6L_{12}(NO_3)_6]^{6+}$. The structures of all the complexes were modelled using DFT calculations. Finally, the challenges and conclusions in determining the specific structural identity of these unsymmetric species are discussed.

Introduction

Nature creates various substantial and complex supramolecular self-assemblies using chiral and unsymmetric components. Even for the obvious importance of understanding these processes, the area of using natural compounds as building blocks in supramolecular chemistry is not extensively explored. There are just a few known synthetic coordination assemblies built of ligands containing small terpenoids,[1] peptides,[2] cyclodextrins,[3–5] or quite recently using bile acids.[6–8]

The self-assembly of organic ligands and metal centers—of which transition-metal cations are frequently used—leads to distinct metallosupramolecular structures such as dimeric or multimeric capsules, molecular polyhedra, metallacycles, interlocked structures, or metallopolymers such as metal–organic frameworks.[9–17] The self-assemblies derived from Pd(II) salts have rich history and their development is continuously progressing.[9–11,15] However, most of metallosupramolecular architectures are highly symmetric as being built of symmetric ligands. The field of low-symmetry supramolecular species is still in its infancy but it has gained more and more attention lately.[18]

The biggest challenge in the synthesis of complexes from unsymmetric coordination ligands is the limited control over the ligand's relative orientation in the self-assembly which can lead to a mixture of many constitutional isomers of the assembly, e.g., Pd_2L_4 can be present in the form of 4 isomers, Pd_3L_6 as 9, Pd_4L_8 as 35, and Pd_6L_{12} even as 112 isomers (excluding their enantiomers). The process of unsymmetric ligand self-assembly into a limited number of isomers,

[*] Dr. O. Jurček
Department of Natural Drugs, Faculty of Pharmacy, Masaryk University
Palackého 1946/1, CZ-61200 Brno, Czechia
E-mail: 239999@mail.muni.cz

Dr. O. Jurček, MSc. S. Chattopadhyay, MSc. P. Radiměřský, Prof. Dr. R. Marek
Department of Chemistry, Faculty of Science, Masaryk University
Kamenice 5, CZ-62500 Brno, Czechia

Dr. O. Jurček, MSc. S. Chattopadhyay, Dr. P. Jurček, Prof. Dr. R. Marek
CEITEC—Central European Institute of Technology, Masaryk University
Kamenice 5, CZ-62500 Brno, Czechia

Dr. E. Kalenius, Dr. A. Kiesilä
Department of Chemistry, University of Jyvaskyla
P. O. Box 35, FI-40014 Jyväskylä, Finland

Dr. J. M. Linnanto
Institute of Physics, University of Tartu
W. Ostwald Street 1, 50411, Tartu, Estonia

preferably a single one, is described as "orientational self-sorting".[19] Other challenge in this area is the accurate determination of molecular structure of these coordination products which can be done either by a combination of analytical methods such as NMR spectroscopy, mass spectrometry (MS), and molecular modelling,[6] or the most reliably by X-ray crystallography.[19,20] Ion mobility mass spectrometry (IM–MS) can further provide information on conformational dynamics and structural and/or conformational monodispersivity. In some cases, IM–MS can reveal the existence of higher nuclearity complexes that are not possible to be observed in mass spectra owing to their low abundance and overlapping *m/z* values.[21,22]

Smallest Pd_2L_4 low-symmetric assemblies are the most studied species so far.[7,23–28] Larger Pd_3L_6 complexes (often referred to as double-walled triangles) prepared of unsymmetric ligands were introduced by Jurček et al. in 2015,[6] since then there are two other examples.[8,29] So far, there are two different structural organizations described for Pd_4L_8, tetrahedral[19] or double-walled square[29,30] built of unsymmetric ligands. There are Pd_5L_{10} complexes built of a symmetric ligand either via guest-adaptive self-assembly[31] or recently without the use of a template.[32] There is no Pd_5L_{10} built of unsymmetric ligand. Finally, there is a number of examples of large coordination Pd_6L_{12} species built of ditopic symmetric ligands forming mostly octahedral,[20,33–44] but also crown-like macrocyclic[31,45] assemblies. Out of these, there is only one example of octahedral Pd_6L_{12} complex assembled of low-symmetry achiral ligand (Figure 1a) by Severin et al.[19]

The bile acids (BAs) are amphiphilic triterpenoids with rigid lipophilic core decorated by variable number of hydroxyl groups on their concave hydrophilic α-side and a flexible alkyl chain bearing carboxylic acid. Their main physiological function is in mediating absorption and transport of lipids and lipid soluble nutrients from digestive tract, but there is an increasing evidence that their physiological importance goes further than just that.[46] BAs found their applications in supramolecular chemistry because of their structural features, reactivity, and physicochemical properties,[47–50] but it was not until recently, that they were introduced to coordination supramolecular chemistry.[6] We demonstrated that ditopic pyridyl ligands derived from ursodeoxycholic acid (UDCA) can form in a narcissistic way large, chiral, concave, supramolecular Pd_3L_6 macrotetracycles with Pd(II) of square planar coordination geometry.[6,8] We have further shown that by using an amphiphilic UDCA-bispyridyl-carboxylic tritopic ligand we can induce self-organization of Pd_3L_6 into microscopic hexagonal particles upon addition of water to its DMSO solution.[8] In this article we introduce a new epimeric BA as a building block in coordination supramolecular chemistry—chenodeoxycholic acid (CDCA). The only structural difference between both 3,7-dihydroxy BAs, the UDCA and the CDCA (ligands derived shown in Figure 1b), is in spatial orientation of the hydroxyl at position C-7, equatorial or axial, respectively. This leads to a difference in bend angle enclosed between OH@C3–C5-OH@C7, i.e., 110° (UDCA) or 90°(CDCA). Therefore, the CDCA-bispyridyl ligand provides new geometric features which can lead to different complexes than known Pd_3L_6. This was indeed confirmed in our experiments revealing a mixture of larger complexes including the superchiral Pd_6L_{12} containing 120 chiral centers. Such chiral density has never been contained in a single artificial metallosupramolecular species. The ligand flexibility and with that connected structural variability of self-assemblies derived from UDCA- and CDCA-bispyridyl ligands is discussed. The study also opens an important chapter of structural predictability of complexes made of flexible, bulky, unsymmetric, and chiral ligands, and further provides an insight into a mechanism of selectivity of orientational self-sorting.

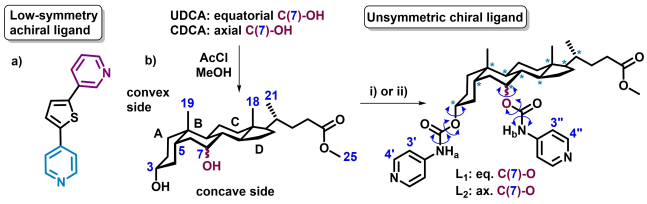

Figure 1. a) Structure of low-symmetry ligand by Severin et al.[19] b) Reaction Scheme of the preparation of the ligands by two pathways: i) triphosgene, 4-aminopyridine, pyridine, DCM; ii) isonicotinoyl azide, toluene. The chemical formulae and partial proton numbering of unsymmetric ligands $\mathbf{L_1}$ (UDCA-based) and $\mathbf{L_2}$ (CDCA-based) are shown. Blue asterisks mark stereocenters which are similar in both BAs (10 in total). Blue arrows indicate rotational flexibility of the ligands. Letters A–D denote rings of the steroid skeleton.

Results and Discussion

The bispyridyl ligands derived from ursodeoxycholic ($\mathbf{L_1}$) and chenodeoxycholic ($\mathbf{L_2}$) bile acid (Figure 1b) were prepared in two steps. The carboxylic acid group of BAs was converted into methyl ester followed by transformation of hydroxyl groups into carbamoyl pyridines. The carbamates were formed either via triphosgene reaction pathway or via isonicotinoyl azide pathway (for details, see Supporting Information). The triphosgene pathway, reported previously,[6,8] provided higher yields for $\mathbf{L_1}$ (45 % vs. 37 %), whereas isonicotinoyl azide pathway provided higher yields for $\mathbf{L_2}$ (30 % vs. 42 %).

In general, a ligand ($\mathbf{L_1}$ or $\mathbf{L_2}$) was dissolved in DMSO-d_6 and the resulting 10 mM solution was used to dissolve $Pd(NO_3)_2{\cdot}2H_2O$ (L:M ratio 2:1). The mixture was heated for 1 h at 55 °C. The course of the complexation reaction was followed using ^{1}H NMR spectroscopy (Figure 2). The complexation of $\mathbf{L_1}$ leads to a deshielding and broadening of the carbamate –NH– and pyridyl H3′, H3″ atoms and a slight shielding of pyridyl H4′, H4″ atoms, which was attributed to a formation of $Pd_3(\mathbf{L_1})_6$ complex (Figure 2a, 2b). The complex and $\mathbf{L_1}$ have the same number of ^{1}H NMR signals, indicating that the supramolecular assembly is formed spontaneously in symmetric and precise manner.

In theory, there can be 9 possible constitutional isomers of Pd_3L_6, but often only the thermodynamically most stable

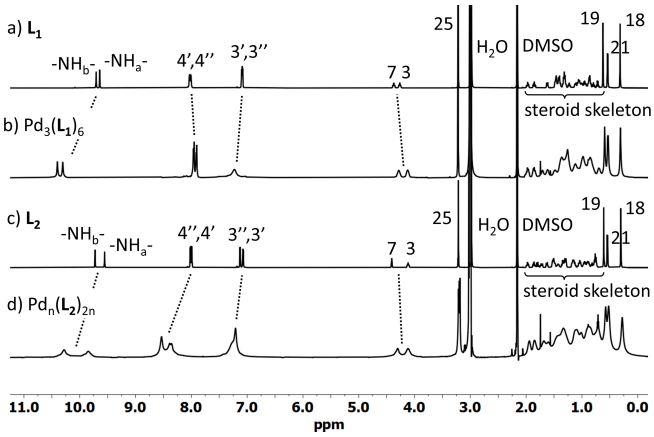

Figure 2. ^{1}H NMR spectra of a) ligand $\mathbf{L_1}$, b) $Pd_3(\mathbf{L_1})_6$, c) ligand $\mathbf{L_2}$, and d) mixture of Pd^{2+}-$\mathbf{L_2}$ complexes.

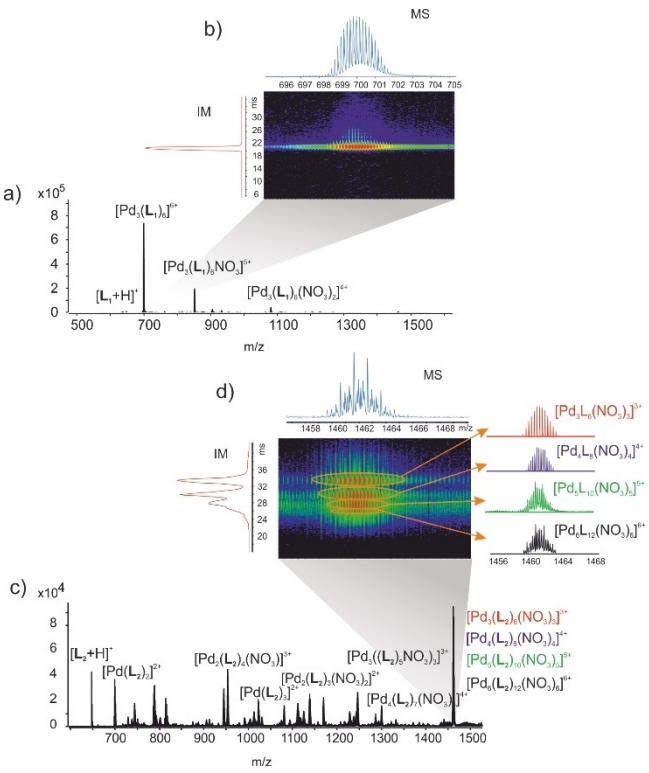

Figure 3. Comparison of the ESI-MS spectra and ion-mobility arrival time distributions for spectra measured from $\mathbf{L_1}$-Pd(II) and $\mathbf{L_2}$-Pd(II) complexation reactions. a) ESI-MS spectrum of $\mathbf{L_1}$-Pd(II) complexation showing exclusive formation of $Pd_3(\mathbf{L_1})_6$, b) ion-mobility arrival time distribution and heat plot for the $[Pd_3(\mathbf{L_1})_6]^{6+}$ ion, c) ESI-MS spectrum of $\mathbf{L_2}$-Pd(II) complexation showing the formation of a variety of Pd(II) complexes, and d) ion-mobility arrival time distribution and heat plot for the ion at *m/z* 146, which is shown to consist of a mixture of $[Pd_3(\mathbf{L_2})_6(NO_3)_3]^{3+}$, $[Pd_4(\mathbf{L_2})_8(NO_3)_4]^{4+}$, $[Pd_5(\mathbf{L_2})_{10}(NO_3)_5]^{5+}$, and $[Pd_6(\mathbf{L_2})_{12}(NO_3)_6]^{6+}$.

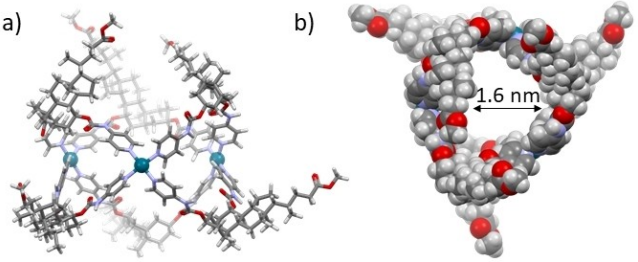

Figure 4. a) Optimized (CAM-B3LYP with SCRF methanol model and LANL2DZ + 6-311G(d,p) method) molecular model of the crown-like $Pd_3(\mathbf{L_1})_6$ complex (side view) and b) top view of complex shown with a CPK model.

one is formed via the orientational self-sorting and can be detected in the reaction mixture.[19] As we elaborately discussed and studied previously using structurally similar ligands derived from the UDCA (Figure S15, C-24 was either benzyl ester or carboxylic acid, while in here it is the methyl ester),[6,8] based on the ^{1}H NMR analysis of the $\mathbf{L_1}$ complex we can assume that the final self-assembly is symmetric. The stoichiometry of the complex was determined by ESI-Q-TOF MS as $Pd_3(\mathbf{L_1})_6$ (Figure 3), further suggesting C_3 rotational symmetry.

Such complex can be represented by two possible constitutional isomers—crown- (Figure 4, previously called "flower"[6,8]) or barrel-like complex, where the six ligands are interconnected by three square-planar Pd(II) centers (PdN_4 coordination sphere). The $Pd_3(\mathbf{L_1})_6$ complex can be divided into a top and a bottom part by an imaginary plane going through the Pd(II) centers. Each part contains three ligands interconnected into a cycle with connectivity (C7-pyridyl)-Pd(II)-(C3-pyridyl), i.e., 7-Pd-3. This top and bottom cycles differ in their orientation to each other in the crown- and the barrel-form, i.e., both cycles travel in the same direction (crown, 7,7-Pd-3,3 coordination sphere) (Figure 4, Scheme 1) or in the opposite direction (barrel, 7,3-Pd-3,7 coordination sphere) (Figure S32).

This was further confirmed by performing a logical structure-transformation analysis (Scheme 1). The principle of the analysis consists in the preparation of trimeric macrocycles by addition of tetrabutylammonium chloride (TBACl) and analysis of the products. The hypothesis is that direct deconstruction of the crown-like $Pd_3(\mathbf{L_1})_6$ using TBACl leads to a single constitutional crown-like isomer $Pd_3(\mathbf{L_1})_3Cl_6$ (also referred to as *cis*), while the same deconstruction of the barrel-like $Pd_3(\mathbf{L_1})_6$ complex leads to two constitutional isomers, the crown-like and an upturned one (also referred to as *trans*) (Scheme 1), which shall be possible to follow using ^{1}H- and ^{1}H DOSY NMR.

As expected, the ^{1}H NMR spectrum of the TBACl reaction shows a new single set of signals of coordinated $\mathbf{L_1}$, next to a signal of free ligand $\mathbf{L_1}$. The chemical shifts are different to those of $Pd_3(\mathbf{L_1})_6$ confirming quantitative formation of a new single coordination product $Pd_3(\mathbf{L_1})_3Cl_6$ (Figure S35). The ESI-MS analysis of the experiment shows presence of $[(\mathbf{L_1})_3Pd_2Cl_4Na]^+$ or $[(\mathbf{L_1})_3Pd_2Cl_3]^+$ ions confirming the expected progress of the reaction towards the formation of a zero net charge $Pd_3(\mathbf{L_1})_3Cl_6$ complex (thus not directly observable by MS). These results confirm that treatment of the C_3-symmetric crown-like complex $Pd_3(\mathbf{L_1})_6$

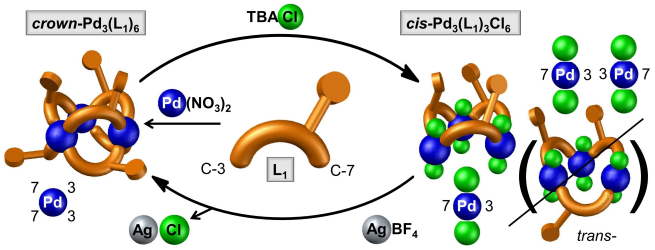

Scheme 1. Structure-transformation analysis: reversible conversion reaction between $Pd_3(\mathbf{L_1})_6$ and trimeric $Pd_3(\mathbf{L_1})_3Cl_6$ species suggesting the existence of a crown-like architecture.

leads to another C_3-symmetric crown-like complex $Pd_3(\mathbf{L_1})_3Cl_6$. Moreover, the original crown-like $Pd_3(\mathbf{L_1})_6$ can be fully recovered from this mixture by AgCl treatment and heating at 55 °C, as confirmed by ^{1}H NMR spectroscopy and MS.

In the following step, all reaction products were studied by ^{1}H DOSY NMR spectroscopy. The diffusion coefficient for the single hexameric species $Pd_3(\mathbf{L_1})_6$ is $D = 7.17\times10^{-11}$ m^2/s (Figure 5a, considering its roughly spherical shape corresponding to 3.4 nm hydrodynamic radius). The *cis*-form of $Pd_3(\mathbf{L_1})_3Cl_6$ provided $D_{cisT} = 7.83\times10^{-11}$ m^2/s (Figure S36, corresponding roughly to 3.1 nm radius). This is consistent with the *cis*- rather than the *trans* isomer, as it was also confirmed by comparison with measurements of their molecular models, which show a diameter 3.6 and 4.4 nm, respectively (Figure S34).

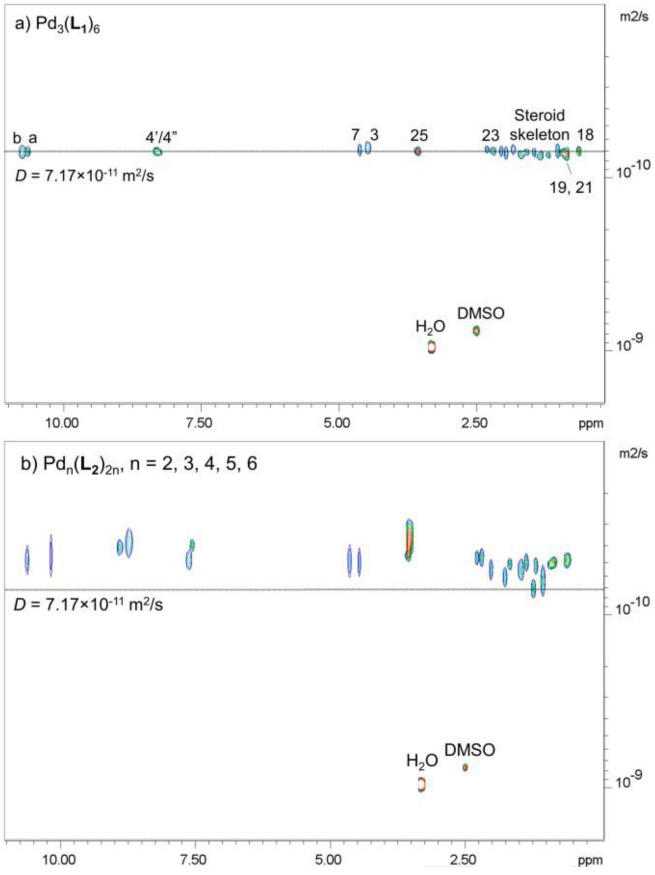

Figure 5. ^{1}H DOSY NMR spectrum (700 MHz, DMSO-d_6, 303 K) of a) $Pd_3(\mathbf{L_1})_6$ ($D = 7.17\times10^{-11}$ m^2 s^{-1}), b) $Pd_n(\mathbf{L_2})_{2n}$, where $n = 3$, 4, 5, or 6, showing multiple species in the reaction mixture (the reference line is set for comparison at $D = 7.17\times10^{-11}$ m^2 s^{-1}, which corresponds to $Pd_3(\mathbf{L_1})_6$).

Another evidence of the presence of the crown-like self-assembly was obtained by ^{1}H–^{1}H NOESY NMR analysis of the $Pd_3(\mathbf{L_1})_6$ solution (Figure S33). The analysis of the spectrum reveals strong interaction of C25-methyl group of ester on the flexible alkyl side chain with multiple protons of the steroid nucleus (including the interaction with methyls C18, C19, and C21) and a weak interaction with pyridylcarbamates. This can be seen as "tapping" of the C25-methyl on the convex face of the above lying neighboring steroid ligand which can only be possible in the crown-like assembly. In contrast, the C25-methyls in the barrel-like assembly point outwards the central Pd-plane of the $Pd_3(\mathbf{L_1})_6$ complex and thus have no possibility for measurable ^{1}H–^{1}H dipolar (NOE) interaction with other neighboring ligands.

The comparison of the collision cross-section (CCS) of the crown-like $Pd_3(\mathbf{L_1})_6$ with the previously published similar Pd_3L_6 self-assemblies further confirms the presence of the crown-like structure. The crown-like complexes of the general formula $[Pd_3(L)_6]^{6+}$ are represented by $^{DT}CCS_{N2}$ 1106–1191 Å^2 for the largest UDCA-based "waving" ligand (Figure S15a),[6] 919.4 Å^2 for the smallest ligand (Figure S15b),[8] and 973.7 Å^2 using the current medium-sized ligand $\mathbf{L_1}$.

Finally, the comparison of the ground state energies of optimized molecular models of $[Pd_3(\mathbf{L_1})_6(NO_3)_3]^{3+}$ shows an energy difference of 10 kcal.mol^{-1} in favor of the crown-like model (yet the energy difference can slightly differ in relation to the position of nitrate anions surrounding the Pd^{2+} center). The reasons for the crown-like architecture are likely encompassed in the ligand's amphiphilic character and natural tendency of BAs to undergo aggregation in polar environment, which together with the relatively flexible binding sites provide conditions for orientational self-sorting into a single constitutional complex crown-$Pd_3(\mathbf{L_1})_6$.

In the case of $\mathbf{L_2}$ complexation, the ^{1}H NMR spectrum of the resulting reaction mixture shows complete coordination of the ligand as seen by signal broadening, but this reaction results in a mixture of coordination complexes (Figure 2d). At least two different sets of overlapping pyridyl signals can be recognized in the spectrum, suggesting the presence of at least two different coordination species or constitutional isomers (similar observation where constitutional isomers could be distinguished based on ^{1}H NMR spectra was previously shown[6]). The ^{1}H resonances of the carbamate –NH– groups and pyridyl H3′, H3″ atoms are shifted to higher frequencies. It is also noteworthy that H4′, H4″ atoms are deshielded in contrast to those in $\mathbf{L_1}$. To induce orientational self-sorting process and selectivity of the reaction of Pd(II) with $\mathbf{L_2}$ we screened different conditions (varying solvent system (Figure S37), temperature) and used different palladium salts (Figure S38), but the reactions generally led

to even more complex mixtures and insoluble precipitates. Moreover, we also tested another approach, where, in the first step, a reaction of $\mathbf{L_2}$ with $PdCl_2$ led to a mixture of fewer coordination products of a general formula $Pd_n(\mathbf{L_2})_nCl_{2n}$, and in the second step reaction with $AgBF_4$ was expected to lead to a simpler mixture of products with general formular $Pd_n(\mathbf{L_2})_{2n}$, but, again, this was not the case (Figure S38d,e, Figure S39).

The mixture from the reaction with $Pd(NO_3)_2$ was analyzed by ESI-MS followed by IM-MS (Figure 3c). The ESI-MS analysis of the $\mathbf{L_2}$-Pd(II) complexation reaction confirmed a mixture of several products. Ions of various stoichiometry were assigned to, e.g., $[Pd_2(\mathbf{L_2})_4(NO_3)]^{3+}$, $[Pd_2(\mathbf{L_2})_3(NO_3)_2]^{2+}$, $[Pd_3(\mathbf{L_2})_5(NO_3)_3]^{3+}$, $[Pd_4(\mathbf{L_2})_7(NO_3)_4]^{4+}$, or a signal with *m/z* 1461 corresponding to $[Pd_3(\mathbf{L_2})_6(NO_3)_3]^{3+}$, but possibly also to larger overlapping species like $[Pd_4(\mathbf{L_2})_8(NO_3)_4]^{4+}$, $[Pd_5(\mathbf{L_2})_{10}(NO_3)_5]^{5+}$, or even $[Pd_6(\mathbf{L_2})_{12}(NO_3)_6]^{6+}$ (Table S1). Arrival time distribution (ATD) separation at *m/z* 1461, indeed, reveals four different ions of $[Pd_3(\mathbf{L_2})_6(NO_3)_3]^{3+}$, $[Pd_4(\mathbf{L_2})_8(NO_3)_4]^{4+}$, $[Pd_5(\mathbf{L_2})_{10}(NO_3)_5]^{5+}$, and $[Pd_6(\mathbf{L_2})_{12}(NO_3)_6]^{6+}$ (Figure 3d).

The size and number of supramolecular self-assemblies of $\mathbf{L_2}$ were also followed using ^{1}H DOSY NMR spectroscopy. The spectrum (Figure 5b) shows a mixture of complexes which are similar or larger than the $Pd_3(\mathbf{L_1})_6$ self-assembly.

Despite many attempts to obtain single crystals of $\mathbf{L_1}$ or $\mathbf{L_2}$ complexes for X-ray diffraction structural analysis, we were not successful. Therefore, the structures of $\mathbf{L_2}$ complexes were also modelled and optimized by DFT calculations. In theory, these complexes can undertake shapes of macrocycles, but in some cases, based on their stoichiometry, they could also form distinct cages, or even interlocked structures. $Pd_3(\mathbf{L_2})_6$ (Figure 6a, S41a) can contain a crown-like macrocycle similar to that of $Pd_3(\mathbf{L_1})_6$. This was also suggested by the comparison of ground state energies of their optimized molecular models of $[Pd_3(\mathbf{L_2})_6(NO_3)_3]^{3+}$, where the difference 10 kcal.mol^{-1} was similarly in favor of the crown-like model compared to the barrel-like isomer. On the other hand, the $Pd_4(\mathbf{L_2})_8$ complex can form either a macrocycle (Figure 6b) or a tetrahedral self-assembly (Figure S42). The $Pd_5(\mathbf{L_2})_{10}$ complex is contained into only possible macrocyclic structure (Figure 6c). And the largest of them all, $Pd_6(\mathbf{L_2})_{12}$, can form a macrocycle (Figure 6d), a cuboid structure (Figure S42), or even mechanically interlocked structure made of two $Pd_3(\mathbf{L_2})_6$ macrocycles.

In the next step, based on the models we calculated theoretical values of CCS and compared them with the experimental ones. IM–MS experiments provide $^{DT}CCS_{He}$ values of 905.1 Å^2 and 1206.7 Å^2 for ions $[Pd_3(\mathbf{L_2})_6(NO_3)_3]^{3+}$ and $[Pd_4(\mathbf{L_2})_8(NO_3)_4]^{4+}$, respectively. These have a good correlation to theoretical $^{DTM}CCS_{He}$ values for $[Pd_3(\mathbf{L_2})_6(NO_3)_3]^{3+}$ either 924.7 Å^2 (barrel, Figure S41d) or 949.9 Å^2 (crown isomer, Figure S41a) and for $[Pd_4(\mathbf{L_2})_8(NO_3)_4]^{4+}$ either 1206.8 (tetrahedron) or 1237.7 Å^2 (crown isomer) (Figure S42). The differences between the constitutional isomers are relatively small, which somehow limits the ultimate structural determination (see Table S2 in SI). Yet, the tetrahedral, cuboid, and mechanically interlocked structures are likely not plausible because of the bulkiness of the peripheral areas of the ligand $\mathbf{L_2}$ (ring C and D bearing the alkyl side chain), its flexibility, and conclusions made based on analytical data collected.

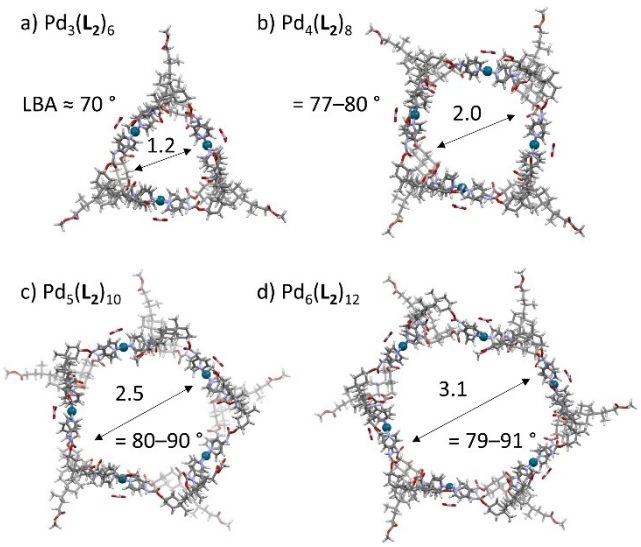

Figure 6. Top view of optimized (CAM–B3LYP with SCRF methanol model and LANL2DZ + 6-311G(d,p) method) molecular models of macrocyclic crown-like complexes: a) triangular $[Pd_3(\mathbf{L_2})_6(NO_3)_3]^{3+}$, b) square $[Pd_4(\mathbf{L_2})_8(NO_3)_4]^{4+}$, c) pentagonal $[Pd_5(\mathbf{L_2})_{10}(NO_3)_5]^{5+}$, and d) hexagonal $[Pd_6(\mathbf{L_2})_{12}(NO_3)_6]^{6+}$ (the cavity diameter is shown in nm, LBA stands for ligand bend angle).

The ^{1}H-^{1}H NOESY NMR analysis of the mixture showed similar interactions as in the case of $Pd_3(\mathbf{L_1})_6$ of the C25-methyl group of ester and protons of the steroid nucleus and pyridylcarbamates confirming the crown-like architecture for the complexes (Figure S40).

Finally, the chirality of the ligands $\mathbf{L_1}$, $\mathbf{L_2}$, and their complexes was studied by electronic circular dichroism (CD) (Figure 7). In general, the change of the CD signals of complexes compared to their ligands suggests that the dichroism is mainly related to structural organization of the complexes mediated through metal to ligand coordination. The experimental results obtained correspond to those previously published for the crown-like Pd_3L_6 complexes[6,8] confirming similar crown-like isomerism. Nevertheless, this seems to be more relevant for the spectrum of $Pd_3(\mathbf{L_1})_6$ where, at the same concentration of the ligand complexed, the signal intensity is higher than the one in the case of complexes made of $\mathbf{L_2}$. The lower signal intensity of the mixture of $Pd_n(\mathbf{L_2})_{2n}$ complexes could further suggest that slight differences in structural organization are present within the mixture. We presume that while the organization of the ligands in $Pd_3(\mathbf{L_1})_6$ follows ideally the 7-Pd-3 directionality of the crown-like self-assembly (7,7-Pd-3,3 coordination sphere), the $Pd_n(\mathbf{L_2})_{2n}$ complexes might contain structural discrepancies from the crown-like architecture and thus provide less optically active species. These structural aberrations could easily be possible for the smaller macrocycles, e.g., $Pd_3(\mathbf{L_2})_6$, where the steric hindrance plays

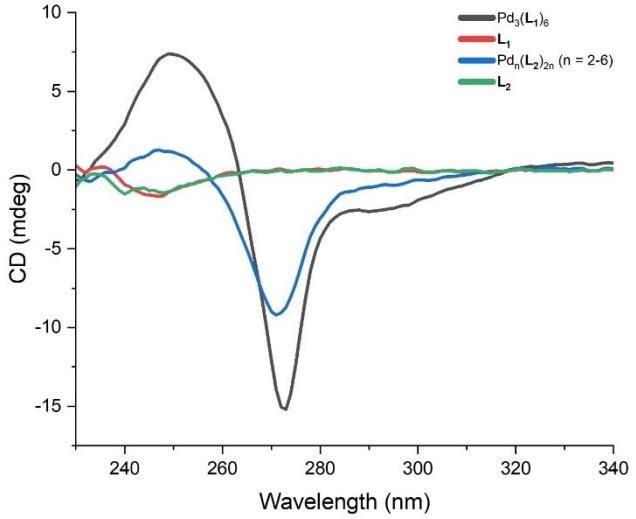

Figure 7. Comparison of electronic circular dichroism spectra of ligand $\mathbf{L_1}$, $\mathbf{L_2}$, $Pd_3(\mathbf{L_1})_6$, and $Pd_n(\mathbf{L_1})_{2n}$, (where $n=2$–6) ($c=10$ μM with respect to ligand, $t=25$ °C, mixture of methanol and DMSO-d_6 in 1000 : 1 ratio).

larger role in orientational self-sorting as the intramolecular distances between ligands are smaller (Figure S41).

In general, the exact structural determination of coordination products with unsymmetric and flexible ligands is challenging (if not being supported by a crystal structure), especially, if the subject of the analyses is an unresolvable mixture of products as in our case. Therefore, new analytical strategies need be developed. Over the years, various strategies have been described in design and analyses of 2D and 3D metallosupramolecular architectures using symmetric ligands, where directional bonding, symmetry interaction, or molecular paneling approaches are the most extensively used and adopted.[51,52] The key factors to be considered in the coordination self-assembly processes are ligand's geometry, its bend angle, structural rigidity/flexibility, and coordination sphere of the metal center.

It is noteworthy, that while in the metallosupramolecular chemistry of symmetric and rigid ligands a general rule applies where the larger is the bend angle the larger is the resulting self-assembly,[52–55] herein it follows rather opposite trend. Nevertheless, this rule seems to be mainly applicable in the construction of coordination cages or polyhedra and might not hold strong for the formation of metalla-cycles.

Introducing the unsymmetric, flexible, but also bulky bile-acid-based ligands brings other structural features. Herein, we investigate and compare them for the ligands $\mathbf{L_1}$ and $\mathbf{L_2}$. DFT calculation of an equilibrium geometry of $\mathbf{L_1}$ (ground state in gas phase using B3LYP/6-31G*) provided a model enclosing 117° bend angle between pyridyl N@C3–C5-pyridyl N@C7 atoms (Figure S1c). Moreover, previously, we could also observe other conformational isomers found in a crystal structure of similar UDCA-based ligand, where four ligand molecules of an asymmetric unit enclose 112, 115, 137, and 145° bend angle (Figure S14, this shall be taken carefully considering crystal constraints).[8] Furthermore, the bend angle of $\mathbf{L_1}$ was measured in the optimized molecular model of $Pd_3(\mathbf{L_1})_6$ where it ranges from 89 to 105°. Overall, this represents quite a large flexibility of $\mathbf{L_1}$ bend angle between 89–145° (Δ56°), and if excluding the bend angles observed in the solid state, 89–117° (Δ28°).

On the other side, the CDCA-based ligand $\mathbf{L_2}$ possesses 72° bend angle in its equilibrium geometry (Figure S16c). The ligand's bend angle was further measured in molecular models of all coordination species, for $Pd_2(\mathbf{L_2})_4$ ranging 42–44°, macrocyclic $Pd_3(\mathbf{L_2})_6$ around 70°, macrocyclic $Pd_4(\mathbf{L_2})_8$ 77–80°, tetrahedral $Pd_4(\mathbf{L_2})_8$ 73–86°, macrocyclic $Pd_5(\mathbf{L_2})_{10}$ 80–90°, macrocyclic $Pd_6(\mathbf{L_2})_{12}$ 79–91°, and cuboid $Pd_6(\mathbf{L_2})_{12}$ 92–105°. Overall, ranging between 42–90° (Δ48°), or when excluding the less abundant or less probable cases of $Pd_2(\mathbf{L_2})_4$ and cuboid $Pd_6(\mathbf{L_2})_{12}$, 70–90° (Δ20°). Comparing the overall bend angles of both ligands, the $\mathbf{L_1}$ roughly covers the range 90–120° (30°) while the $\mathbf{L_2}$ covers the range 70–90° (20°), making them geometrically complementary building blocks. It appears that the higher is the flexibility of the unsymmetric ligand the higher is the probability of its orientational self-sorting into a single product.

The molecular modelling has further shown that not only bending of flexible ligands' moieties is responsible for their flexibility, but also the rotation around the C3–CO–NH-pyridine axis plays an important role. Especially for $\mathbf{L_2}$, the rotational freedom around the axis supplies to some extent the ligands' structural limitations given by a narrower bend angle. In connection to this, small energetical variability was also observed when comparing various conformational species of the crown-like $Pd_3(\mathbf{L_2})_6$ complexes. The differences in carbamate-pyridyl orientations additionally vary the overall size of the whole $Pd_3(\mathbf{L_2})_6$ complex, i.e., when all protons of –NH– group point away from the C3 axis the Pd–Pd distance in the complex is about 0.5–1 Å larger than that of the complex where one of the hydrogen –NH– atom points towards the C3 axis (or towards the C7). This size variability can also be somehow supported by a slightly broader ATD for $[Pd_3(\mathbf{L_2})_6(NO_3)_3]^{3+}$ in IM-MS (which can also be seen as another manifestation of "tapping" C25 methyl as observed by NOESY NMR).

Moreover, if we only consider the comparable species Pd_3L_6, the bend angle of $\mathbf{L_1}$ in $Pd_3(\mathbf{L_1})_6$ complex ranges between 89–105°, while the bend angle of $\mathbf{L_2}$ in $Pd_3(\mathbf{L_2})_6$ is limited to about 70° suggesting structural rigidity and increased tension in the latter one. This is making it energetically less favorable product, which ultimately can be the reason for structural preferences of $\mathbf{L_2}$ towards rather looser and larger macrocyclic species, where the bend angle can slightly vary. It also appears that $\mathbf{L_1}$ feels lesser steric hindrance when being assembled in the complex because of different orientation of the side chain with C and D steroid rings. Indeed, the difference in ligands' bulkiness can be observed from the comparison of the molecular models of $\mathbf{L_1}$ and $\mathbf{L_2}$ (Figure S44). In case of $\mathbf{L_2}$, the volume of C+D-moiety extends in one direction over the length of steroidal A and B rings bearing the pyridyl binding sites. This structural organization could be sterically limiting the orientational self-sorting and self-assembly into regular crown-like architecture and thus causing suggested structural

aberrations (some possible constitutional isomers of $Pd_3(\mathbf{L_2})_6$ are shown in Figure S41).

Conclusion

Herein, we introduced chenodeoxycholic acid (CDCA) as a core unit of the bispyridyl ligand to be used in metallosupramolecular chemistry. A comparison to the known framework of ursodeoxycholic acid (UDCA) is presented with a focus on differences in their molecular structure and resulting Pd(II) macrocycles. In general, both ligands provide macrocyclic structures. While the UDCA ligand leads selectively via orientational self-sorting to a single constitutional isomer of Pd_3L_6, the CDCA ligand results in a mixture of mostly larger macrocyclic complexes Pd_nL_{2n}, starting from Pd_2L_4 all the way up to a giant Pd_6L_{12}.

The lack of symmetry, bulkiness, and partial flexibility of the ligands might, at first, rather complicate the prediction of their final self-assemblies, yet once some systematic structural code is unveiled, it leads to a general better understanding of the important self-assembly behavior of unsymmetric, chiral and flexible building blocks with a relevance to natural processes (yet still much more complex). The elemental rules of ligand bend angle, rigidity, and metal geometry can be a good starting point when working with ligands slightly diverging from the symmetry. Nevertheless, several other features need to be considered when explaining the orientational self-sorting of truly unsymmetric ligands like ours, such as flexibility of bend angle, directionality, and steric requirements, together with natural propensity of BAs to aggregate because of their amphiphilic character. The logical structure-transformation analysis as we introduced serves well as a method for structural confirmation. Also, CD spectroscopy might represent an important new approach for structural characterization of supramolecular self-assemblies composed of chiral unsymmetric coordination ligands and it can also serve well in the description of their regularity.

There is an intriguing orientational self-sorting when using $\mathbf{L_1}$, a feature which can now be related to the ligand's optimal bend angle, flexibility, and distribution of bulkiness. On the other hand, there is a general specificity mounted in the bile acid skeleton, as also shown when using $\mathbf{L_2}$, steering the course of coordination self-assembly preferably towards the crown-like macrocyclic complexes, yet in this case of varying size.

Moreover, the spatial orientation of hydroxyl groups at C-3 and C-7 of CDCA are the same as in the molecule of cholic acid—the least toxic and the most water-soluble bile acid commercially available, which predestines its similar utilization in coordination supramolecular chemistry. High level of chiral density of these macrocyclic complexes is another interesting feature with possible future applications, e.g., in enantioselective catalysis, or in mediation of chiral recognition and enantioselective separations.

Supporting Information

The authors have cited additional references within the Supporting Information.[54–59]

Acknowledgements

We thank Dr. Miroslava Bittová and Dr. Antonín Bednařík for measuring some of the MS spectra. This project has received funding from the European Union's Horizon 2020 research and innovation programme under the Marie Skłodowska-Curie and is co-financed by the South Moravian Region under grant agreement No. 665860 (OJ). This publication reflects only the authors' view and the EU is not responsible for any use that may be made of the information it contains. We acknowledge the Czech Science Foundation (Grant No. 24-10760S to R.M.) and the Core Facilities Josef Dadok National NMR Center and Biomolecular Interactions and Crystallography of CIISB, Instruct-CZ Centre, supported by MEYS CR (LM2023042) and the European Regional Development Fund-Project "UP CIISB" (No. CZ.02.1.01/0.0/0.0/18_046/0015974). JML thanks Estonian Research Council (Grant PSG264). Open Access publishing facilitated by Masarykova univerzita, as part of the Wiley - CzechELib agreement.

Conflict of Interest

The authors declare no conflict of interest.

Data Availability Statement

The data that support the findings of this study are available from the corresponding author upon reasonable request.

Keywords: self-assembly · epimerism · chirality · cage compounds · supramolecular chemistry

[1] O. Mamula, *Coord. Chem. Rev.* **2003**, *242*, 87–95.
[2] T. Sawada, M. Fujita, *Chem* **2020**, *6*, 1861–1876.
[3] R. A. Smaldone, R. S. Forgan, H. Furukawa, J. J. Gassensmith, A. M. Z. Slawin, O. M. Yaghi, J. F. Stoddart, *Angew. Chem. Int. Ed.* **2010**, *49*, 8630–8634.
[4] I. Roy, J. F. Stoddart, *Acc. Chem. Res.* **2021**, *54*, 1440–1453.
[5] O. Jurček, R. Puttreddy, F. Topić, P. Jurček, P. Zarabadi-Poor, H. V. Schröder, R. Marek, K. Rissanen, *Cryst. Growth Des.* **2020**, *20*, 4193–4199.
[6] O. Jurček, P. Bonakdarzadeh, E. Kalenius, J. M. Linnanto, M. Groessl, R. Knochenmuss, J. A. Ihalainen, K. Rissanen, *Angew. Chem. Int. Ed.* **2015**, *54*, 15462–15467.
[7] S. K. Sen, R. Natarajan, *Inorg. Chem.* **2019**, *58*, 7180–7188.
[8] O. Jurček, Nonappa, E. Kalenius, P. Jurček, J. M. Linnanto, R. Puttreddy, H. Valkenier, N. Houbenov, M. Babiak, M. Peterek, A. P. Davis, R. Marek, K. Rissanen, *Cell Rep. Phys. Sci.* **2021**, *2*, 100303.
[9] T. R. Cook, P. J. Stang, *Chem. Rev.* **2015**, *115*, 7001–7045.

[10] M. Han, D. M. Engelhard, G. H. Clever, *Chem. Soc. Rev.* **2014**, *43*, 1848–1860.
[11] D. Tripathy, N. B. Debata, K. C. Naik, H. S. Sahoo, *Coord. Chem. Rev.* **2022**, *456*, 214396.
[12] L.-J. Chen, H.-B. Yang, M. Shionoya, *Chem. Soc. Rev.* **2017**, *46*, 2555–2576.
[13] M. Pan, K. Wu, J.-H. Zhang, C.-Y. Su, *Coord. Chem. Rev.* **2019**, *378*, 333–349.
[14] S. Pullen, J. Tessarolo, G. H. Clever, *Chem. Sci.* **2021**, *12*, 7269–7293.
[15] R. A. S. Vasdev, D. Preston, J. D. Crowley, *Chem. Asian J.* **2017**, *12*, 2513–2523.
[16] A. M. Spokoyny, D. Kim, A. Sumrein, C. A. Mirkin, *Chem. Soc. Rev.* **2009**, *38*, 1218.
[17] J. E. Beves, B. A. Blight, C. J. Campbell, D. A. Leigh, R. T. McBurney, *Angew. Chem. Int. Ed.* **2011**, *50*, 9260–9327.
[18] J. E. M. Lewis, J. D. Crowley, *ChemPlusChem* **2020**, *85*, 815–827.
[19] R.-J. Li, A. Marcus, F. Fadaei-Tirani, K. Severin, *Chem. Commun.* **2021**, *57*, 10023–10026.
[20] B. Roy, R. Saha, A. K. Ghosh, Y. Patil, P. S. Mukherjee, *Inorg. Chem.* **2017**, *56*, 3579–3588.
[21] E. Kalenius, M. Groessl, K. Rissanen, *Nat. Chem. Rev.* **2019**, *3*, 4–14.
[22] O. H. Lloyd Williams, N. J. Rijs, *Front. Chem.* **2021**, *9*, 682743.
[23] D. Ogata, J. Yuasa, *Angew. Chem. Int. Ed.* **2019**, *58*, 18424–18428.
[24] S. Samantray, S. Krishnaswamy, D. K. Chand, *Nat. Commun.* **2020**, *11*, 880.
[25] S. S. Mishra, S. V. K. Kompella, S. Krishnaswamy, S. Balasubramanian, D. K. Chand, *Inorg. Chem.* **2020**, *59*, 12884–12894.
[26] A. Tarzia, J. E. M. Lewis, K. E. Jelfs, *Angew. Chem. Int. Ed.* **2021**, *60*, 20879–20887.
[27] J. E. M. Lewis, A. Tarzia, A. J. P. White, K. E. Jelfs, *Chem. Sci.* **2020**, *11*, 677–683.
[28] J. E. M. Lewis, *Chem. Eur. J.* **2021**, *27*, 4454–4460.
[29] R. Gupta, H. Paithankar, J. Chugh, R. Boomishankar, *Inorg. Chem.* **2021**, *60*, 10468–10477.
[30] C. Klein, C. Gütz, M. Bogner, F. Topić, K. Rissanen, A. Lützen, *Angew. Chem. Int. Ed.* **2014**, *53*, 3739–3742.
[31] T. Zhang, L.-P. Zhou, X.-Q. Guo, L.-X. Cai, Q.-F. Sun, *Nat. Commun.* **2017**, *8*, 15898.
[32] L. Neukirch, M. D. Kulas, J. J. Holstein, G. H. Clever, *Chem. Eur. J.* **2024**, *30*, e202400132.
[33] C. Gütz, R. Hovorka, C. Klein, Q.-Q. Jiang, C. Bannwarth, M. Engeser, C. Schmuck, W. Assenmacher, W. Mader, F. Topić, K. Rissanen, S. Grimme, A. Lützen, *Angew. Chem. Int. Ed.* **2014**, *53*, 1693–1698.
[34] S. Komine, T. Tateishi, T. Kojima, H. Nakagawa, Y. Hayashi, S. Takahashi, S. Hiraoka, *Dalton Trans.* **2019**, *48*, 4139–4148.
[35] S. M. Jansze, G. Cecot, M. D. Wise, K. O. Zhurov, T. K. Ronson, A. M. Castilla, A. Finelli, P. Pattison, E. Solari, R. Scopelliti, G. E. Zelinskii, A. V. Vologzhanina, Y. Z. Voloshin, J. R. Nitschke, K. Severin, *J. Am. Chem. Soc.* **2016**, *138*, 2046–2054.
[36] P. Howlader, S. Mukherjee, R. Saha, P. S. Mukherjee, *Dalton Trans.* **2015**, *44*, 20493–20501.
[37] L. Zeng, S. Sun, Z.-W. Wei, Y. Xin, L. Liu, J. Zhang, *RSC Adv.* **2020**, *10*, 39323–39327.
[38] D. R. Martir, A. Pizzolante, D. Escudero, D. Jacquemin, S. L. Warriner, E. Zysman-Colman, *ACS Appl. Energ. Mater.* **2018**, *1*, 2971–2978.
[39] X. Tang, H. Jiang, Y. Si, N. Rampal, W. Gong, C. Cheng, X. Kang, D. Fairen-Jimenez, Y. Cui, Y. Liu, *Chem* **2021**, *7*, 2771–2786.
[40] E. O. Bobylev, B. De Bruin, J. N. H. Reek, *Inorg. Chem.* **2021**, *60*, 12498–12505.
[41] K. Suzuki, M. Tominaga, M. Kawano, M. Fujita, *Chem. Commun.* **2009**, 1638.
[42] C. Liu, E. O. Bobylev, Y. Fu, D. A. Poole, K. Robeyns, C. Fustin, Y. Garcia, J. N. H. Reek, M. L. Singleton, *Chem. Eur. J.* **2020**, *26*, 11960–11965.
[43] M. D. Wise, J. J. Holstein, P. Pattison, C. Besnard, E. Solari, R. Scopelliti, G. Bricogne, K. Severin, *Chem. Sci.* **2015**, *6*, 1004–1010.
[44] M. Han, R. Michel, G. H. Clever, *Chem. Eur. J.* **2014**, *20*, 10640–10644.
[45] E. Benchimol, K. E. Ebbert, A. Walther, J. J. Holstein, G. H. Clever, *Chem. Eur. J.* **2024**, e202401850.
[46] R. Durník, L. Šindlerová, P. Babica, O. Jurček, *Molecules* **2022**, *27*, 2961.
[47] J. Tamminen, E. Kolehmainen, *Molecules* **2001**, *6*, 21–46.
[48] Nonappa, U. Maitra, *Org. Biomol. Chem.* **2008**, *6*, 657–669.
[49] H. Svobodová, V. Noponen, E. Kolehmainen, E. Sievänen, *RSC Adv.* **2012**, *2*, 4985–5007.
[50] H. Valkenier, A. P. Davis, *Acc. Chem. Res.* **2013**, *46*, 2898–2909.
[51] R. Chakrabarty, P. S. Mukherjee, P. J. Stang, *Chem. Rev.* **2011**, *111*, 6810–6918.
[52] J. Bunzen, J. Iwasa, P. Bonakdarzadeh, E. Numata, K. Rissanen, S. Sato, M. Fujita, *Angew. Chem. Int. Ed.* **2012**, *51*, 3161–3163.
[53] Q.-F. Sun, J. Iwasa, D. Ogawa, Y. Ishido, S. Sato, T. Ozeki, Y. Sei, K. Yamaguchi, M. Fujita, *Science* **2010**, *328*, 1144–1147.
[54] D. Fujita, H. Yokoyama, Y. Ueda, S. Sato, M. Fujita, *Angew. Chem. Int. Ed.* **2015**, *54*, 155–158.
[55] D. Fujita, Y. Ueda, S. Sato, H. Yokoyama, N. Mizuno, T. Kumasaka, M. Fujita, *Chem* **2016**, *1*, 91–101.
[56] S. M. Stow, T. J. Causon, X. Zheng, R. T. Kurulugama, T. Mairinger, J. C. May, E. E. Rennie, E. S. Baker, R. D. Smith, J. A. McLean, S. Hann, J. C. Fjeldsted, *Anal. Chem.* **2017**, *89*, 9048–9055.
[57] V. Gabelica, A. A. Shvartsburg, C. Afonso, P. Barran, J. L. P. Benesch, C. Bleiholder, M. T. Bowers, A. Bilbao, M. F. Bush, J. L. Campbell, I. D. G. Campuzano, T. Causon, B. H. Clowers, C. S. Creaser, E. De Pauw, J. Far, F. Fernandez-Lima, J. C. Fjeldsted, K. Giles, M. Groessl, C. J. Hogan, S. Hann, H. I. Kim, R. T. Kurulugama, J. C. May, J. A. McLean, K. Pagel, K. Richardson, M. E. Ridgeway, F. Rosu, F. Sobott, K. Thalassinos, S. J. Valentine, T. Wyttenbach, *Mass Spectrom. Rev.* **2019**, *38*, 291–320.
[58] C. Larriba-Andaluz, C. J. Hogan, *J. Chem. Phys.* **2014**, *141*, 194107.
[59] D. Joseph, S. Lee, *Org. Lett.* **2022**, *24*, 6186–6191.
[60] K. L. Stoltz, R. Erickson, C. Staley, A. R. Weingarden, E. Romens, C. J. Steer, A. Khoruts, M. J. Sadowsky, P. I. Dosa, *J. Med. Chem.* **2017**, *60*, 3451–3471.
[61] Q. Li, G. P. Tochtrop, *Tetrahedron Lett.* **2011**, *52*, 4137–4139.

Manuscript received: May 14, 2024
Accepted manuscript online: June 6, 2024
Version of record online: August 1, 2024